frontiers in Immunology

ORIGINAL RESEARCH
published: 26 January 2021
doi: 10.3389/fimmu.2020.602254

Induction of SARS-CoV-2 Protein S-Specific CD8+ T Cells in the Lungs of gp96-Ig-S Vaccinated Mice

Eva Fisher[1], *Laura Padula*[1], *Kristin Podack*[1], *Katelyn O'Neill*[1], *Matthew M. Seavey*[2], *Padmini Jayaraman*[2], *Rahul Jasuja*[2] *and Natasa Strbo*[1]*

[1] Department of Microbiology and Immunology, Miller School of Medicine, University of Miami, Miami, FL, United States, [2] Heat Biologics, Inc., Morrisville, NC, United States

Given the aggressive spread of COVID-19-related deaths, there is an urgent public health need to support the development of vaccine candidates to rapidly improve the available control measures against SARS-CoV-2. To meet this need, we are leveraging our existing vaccine platform to target SARS-CoV-2. Here, we generated cellular heat shock chaperone protein, glycoprotein 96 (gp96), to deliver SARS-CoV-2 protein S (spike) to the immune system and to induce cell-mediated immune responses. We showed that our vaccine platform effectively stimulates a robust cellular immune response against protein S. Moreover, we confirmed that gp96-Ig, secreted from allogeneic cells expressing full-length protein S, generates powerful, protein S polyepitope-specific CD4+ and CD8+ T cell responses in both lung interstitium and airways. These findings were further strengthened by the observation that protein-S -specific CD8+ T cells were induced in human leukocyte antigen HLA-A2.1 transgenic mice thus providing encouraging translational data that the vaccine is likely to work in humans, in the context of SARS-CoV-2 antigen presentation.

Keywords: heat shock protein, glycoprotein 96, vaccine, lungs, COVID-19, SARS-CoV-2 protein S, CD8+ T cells

OPEN ACCESS

Edited by:
Katie Ewer,
University of Oxford, United Kingdom

Reviewed by:
Allan Randrup Thomsen,
University of Copenhagen, Denmark
Salvador Iborra,
Universidad Complutense de Madrid, Spain

***Correspondence:**
Natasa Strbo
nstrbo@med.miami.edu

Specialty section:
This article was submitted to Vaccines and Molecular Therapeutics, a section of the journal Frontiers in Immunology

Received: *02 September 2020*
Accepted: *17 December 2020*
Published: *26 January 2021*

Citation:
Fisher E, Padula L, Podack K, O'Neill K, Seavey MM, Jayaraman P, Jasuja R and Strbo N (2021) Induction of SARS-CoV-2 Protein S-Specific CD8+ T Cells in the Lungs of gp96-Ig-S Vaccinated Mice. Front. Immunol. 11:602254. doi: 10.3389/fimmu.2020.602254

INTRODUCTION

The rapid spread of the global COVID-19 pandemic has put pressure on the development of a SARS-CoV-2 vaccine to address global health concerns. We generated a gp96-Ig-secreting vaccine expressing full-length spike or "S" glycoprotein of SARS-CoV-2 *via* a cell-delivered platform. Targeting SARS-CoV-2 spike (S) protein remains the favorable vaccine choice as it is one of the most abundant and immunogenic proteins translated from the SARS-CoV-2 genome (1). Antibodies targeting S protein aim to neutralize mammalian host-cell interaction, thereby minimizing viral multiplicity of infection, however, recent studies have shown that "antibodies are not enough" to protect against COVID-19 for a variety of reasons, including S-protein glycosylation, which shields the antibody from eliciting an optimal neutralization response (2). Antibody decay has also been detected in individuals after recovery from COVID-19, and this decline was more rapid than reported for the first SARS infection in 2003 (3, 4).

T-cell immunity plays a pivotal role in generating a durable immune memory response to protect against viral infection. Prior studies have shown that memory B-cell responses tend to be short lived

after infection with SARS-CoV-1 (5, 6). In contrast, memory T-cell responses can persist for many years (7). Recent data confirm that SARS-CoV-2-specific memory CD8+ T cells are present in the vast majority of patients following recovery from COVID-19 (7–10), and their protective role has been inferred from studies in patients who have had both SARS and MERS (11–13). Recent reports show that patients who have recovered from a severe SARS-CoV-2 infection have T-cell responses against viral spike protein and other structural and nonstructural proteins; in some patients, T-cell responses were present regardless of symptoms or antibody seropositivity (14–16). Here, we generated a COVID-19 vaccine based on the proprietary secreted heat shock protein, gp96-Ig vaccine strategy, that induces antigen-specific CD8+ T lymphocytes in epithelial tissues, including lungs.

Tissue-resident memory (TRM) T cells have been recognized as a distinct population of memory cells that are capable of rapidly responding to infection in the tissue, without requiring priming in the lymph nodes (17–20). Several key molecules important for CD8+ T cell entry and retention in the lung have been identified (21–26) and recently CD69 and CXCR6 (20, 27–29) have been confirmed as core markers that define TRM cells in the lungs. Furthermore, it was confirmed that CXCR6-CXCL16 interactions control the localization and maintenance of virus-specific CD8+ TRM cells in the lungs (20). It has also been shown that, in heterosubtypic influenza challenge studies (30–32), TRM were required for effective clearance of the virus. Therefore, vaccination strategies targeting generation of TRM and their persistence may provide enhanced immunity, compared with vaccines that rely on circulating responses (32).

Our platform technology consists of a genetically engineered construct of gp96, fusion protein gp96-Ig, wherein the C-terminal KDEL-retention sequence was replaced with the fragment crystallizable (Fc) portion of immunoglobulin G1 (IgG1), and then encoded within a plasmid vector that is transfected into a cell line of interest. The cell serves as the antigen supply to secreted gp96-Ig. Complexes of gp96-Ig and antigenic peptides lead to specific cross-presentation of cell-derived antigens by gp96-Ig *in vivo* (33, 34). A crucial advantage offered by this gp96-based technology platform is that it allows for any antigen (such as SARS-CoV-2 S peptides) in the complex with gp96 to drive a potent and long-standing immune response. Over the last 2 decades, we have established that gp96-Ig, secreted from allogeneic or xenogeneic cells containing selected infectious antigens, generates potent, disease antigen specific, polyepitope, multifunctional CD8+ T cells in epithelial tissues (33–39). Here we generated a COVID-19 vaccine based on the secreted heat shock protein gp96-Ig vaccine strategy, and demonstrated vaccine-induced SARS-CoV-2 protein S-specific CD8+ and CD4+ T lymphocytes in epithelial tissues, including lungs and airways. The secreted gp96-Ig-COVID-19 vaccine has the potential to elicit robust long-term memory T-cell responses against multiple SARS-CoV-2 antigens and is designed to work cohesively with other treatments/vaccines (as boosters or as second-line defense) with large-scale manufacturing potential.

METHODS

Generation of Vaccine Cell Lines

Human embryonic kidney (HEK)-293 cells, obtained from the American Tissue Culture Collection (ATCC, #CRL-1573) and human lung adenocarcinoma cell lines (AD100) (40, 41) (source: University of Miami, FL, USA) were transfected with 2 plasmids: B45 encoding gp96-Ig (source: University of Miami) and pcDNA^{TM} 3.1(–) (Invitrogen), encoding full-length SARS-CoV-2 protein S gene (Genomic Sequence: NC_045512.2; NCBI Reference Sequence: YP_009724390.1 GenBank Reference Sequence: QHD43416). A B45 plasmid expressing secreted gp96-Ig has been approved by the Food and Drug Administration and Office of Biotechnology Activities for human use and is currently employed in a clinical study for the treatment of nonsmall cell lung cancer (NSCLC) (NCT02117024, NCT02439450) (42). The histidinol-selected, B45 plasmid, replicates as multicopy episomes and provides high levels of expression. Full-length SARS-CoV-2 protein S is based upon published SARS-CoV-2 protein S sequence from the original Wuhan strain (GenBank Reference Sequence: QHD43416) and cloned into the neomycin-selectable eukaryotic expression vector, pcDNA 3.1(-). HEK-293 and AD100 cells were simultaneously transfected with B45 and pcDNA 3.1 plasmid by Lipofectamine 3000 (Invitrogen) following the manufacturers' protocols. Transfected cells were selected with 1 mg/ml of G418 (Life Technologies, Inc.) and with 7.5 mM of L-Histidinol (Sigma Chemical Co., St. Louis, MO, USA). After stable transfection, a cell line was established. Single cell cloning by limiting dilution assay was performed, and all the cell clones were first screened for gp96-Ig production and then for protein S expression. Vaccine cells sterility testing and IMPACT^{TM} II polymerase chain reaction evaluation was performed for: Ectromelia, mouse rotavirus (EDIM), lymphocytic choriomeningitis virus (LCMV), lactate dehydrogenase-elevating virus (LDEV), mouse adenovirus (MAV1, MAV2), mouse cytomegalovirus (MCMV), mouse hepatitis virus (MHV), murine norovirus (MNV), mouse parvovirus (MPV), minute virus of mice (MVM), mycoplasma pulmonis, Mycoplasma sp., Polyoma, pneumonia virus of mice (PVM), Reovirus 3 (REO3), Sendai, Theiler's murine encephalomyelitis virus (TMEV). All test results were negative.

Western Blotting and Enzyme-Linked Immunosorbent Assay

Protein expression was verified by SDS-page and Western blotting using rabbit anti-SARS-CoV-2 spike glycoprotein antibody (MBS 150780) at 1/1000 dilution and secondary antibody: Peroxidase AffiniPure F(ab')$_2$ Fragment Donkey Anti-Rabbit IgG (H+L) (Jackson ImmunoResearch Laboratories) horseradish peroxidase conjugated anti-rabbit IgG (Jackson ImmunoResearch) at 1/10,000 dilution. S protein was visualized by an enhanced chemiluminescence detection system (Amersham Biosciences, Piscataway, NJ, USA) (**Figure 1C**). Recombinant human coronavirus SARS-CoV-2 spike glycoprotein S1 (Fc Chimera) (ab272105, Abcam) was used as

positive control (loaded 2.4 ug/lane). One million cells were plated in 1 ml for 24 hours (h) and secreted gp96-Ig production was determined by ELISA using anti-human IgG antibody for detection and human IgG1 as a standard (**Figure 1B**).

Immunofluorescence

AD100-gp96-Ig cytospins were fixed in pure cold acetone (VWR chemicals, BDH®, Catalog #BDH1101) for 10 min followed by three washes of 5 min each with phosphate-buffered saline (PBS). The slides were left in blocking media [5% bovine serum albumin (BSA) in PBS] at room temperature for 2 h. Rabbit anti-SARS-CoV-2 spike glycoprotein antibody (Abcam ab272504) and Donkey anti-rabbit IgG FITC, (BioLegend Cat# 406403) fluorescent antibody—were added in 1/50 and 1/100 dilutions of the antibodies combined in 5% BSA in PBS and/or rabbit isotype control (Abcam Ab172730 diluted 1/50), and incubated overnight at 4° C in a dark moisture chamber. The next day, slides were washed 3 times for 5 min with PBS and mounted with

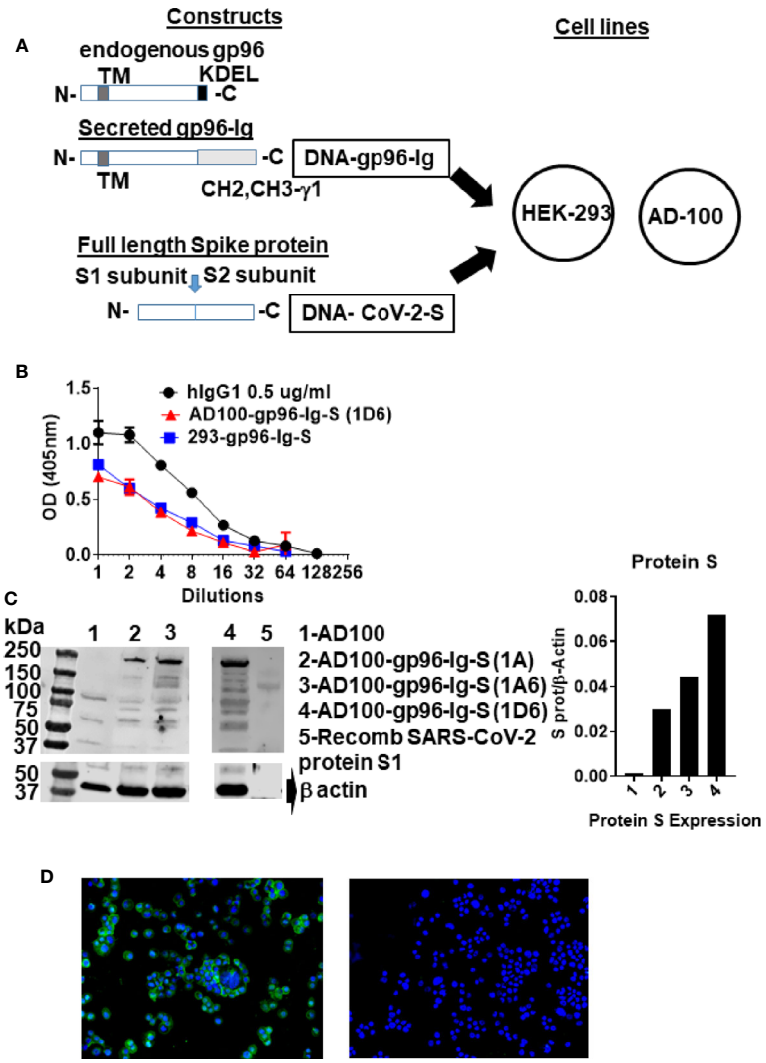

FIGURE 1 | Schematic of gp96-Ig and SARS-CoV-2 protein S constructs used to generate vaccine cells HEK-293-gp96-Ig-S and AD-100-gp96-Ig-S. **(A)** Each panel presents the protein expressed by the DNA (black outline) for the gp96-Ig and SARS-CoV-2 protein S vaccine antigen. Gp96-Ig and SARS-CoV-2-S DNA were cloned into the mammalian expression vectors B45 and pcDNA 3.1, which are transfected into HEK-293 and AD100. Stably transfected vaccine cell clones (1A, 1A6, 1D6) were generated after selection with L-Histidinol and Neomycin; **(B)** One million 293-gp96-Ig-S and AD-100-gp96-Ig-S (1D6) cells were plated in 1 ml for 24 h and gp96-Ig production in the supernatant was determined by ELISA using anti-human IgG antibody for detection with human IgG1 (0.5 ug/ml) as a standard; **(C)** Cell lysates were analyzed under reduced conditions by SDS-PAGE and Western blotting using anti protein S antibody and recombinant protein S1 as a positive control; **(D)** IF for protein S (in green) expressed in AD100-gp96-Ig-S cells using rabbit anti-SARS-CoV-2 S antibody and anti-rabbit Ig-AF488 as secondary antibody. AD100 was used as a negative control and β-actin for protein quantification. Original magnification 40× with DAPI nuclear staining shown in blue. DNA, deoxyribonucleic acid; ELISA, enzyme-linked immunosorbent assay; IgG, immunoglobulin G; N, amino terminus; C, carboxy terminus; IF, immunofluorescence; TM, transmembrane domain; KDEL, retention signal; CH2 CH3 gamma 1, heavy chain of IgG1. See text for explanation.

Prolong Gold antifade reagent with DAPI from Invitrogen (Catalog #36935), covered with a coverslip, and allowed to cure. The slides were then sealed with nail polish and taken to the KEYENCE microscope for examination. The following filter cubes were used: DAPI (for nuclear stain), FITC (for protein S), and images were acquired on KEYENCE microscope (BZ-X Viewer).

Animals and Vaccination

Mice used in this study were colony-bred mice (C57Bl/6) and human leukocyte antigen (HLA)-A02-01 transgenic mice [C57BL/6-Mcph1Tg (HLA-A2.1)1Enge/J, Stock No: 003475] purchased from JAX Mice (the Jackson Laboratory for Genomic Medicine, Farmington, CT, USA). Homozygous mice carrying the Tg (HLA-A2.1)1Enge transgene express human class I major histocompatibility complex (MHC) Ag HLA-A2.1. The animals were housed and handled in accordance with the standards of the Association for the Assessment and Accreditation of Laboratory Animal Care International under University of Miami Institutional Animal Care & Use Committee-approved protocol. Both female and male mice were used at 6–10 weeks of age.

Equivalent number of 293-gp96-Ig-protein S and AD100-gp96-Ig-protein S cells that produce 200 ng gp96-Ig or PBS were injected *via* the subcutaneous (s.c.) route in C57Bl/6 and HLA-A2.1 transgenic mice. Mice received vaccination on days 0 and 30 and were sacrificed 5 and 30 days after vaccination. Spleen, lungs, and bronchoalveolar lavage (BAL) were collected and processed into single-cell suspension.

BAL and Lung Harvest and Cell Isolation

For mouse samples, spleens were collected, and tissues processed into single-cell suspension. Leukocytes were isolated from spleen by mechanical dissociation and red blood cells were lysed by lysing solution. BAL was harvested directly from euthanized mice *via* insertion of a 22-gauge catheter into an incision into the trachea. Hanks' Balanced Salt Solution (HBSS) was injected into the trachea and aspirated 4 times. Recovered lavage fluid was collected and BAL cells were gathered after centrifugation.

To isolate intraparenchymal lung lymphoid cells, the lungs were flushed by 5 ml of prechilled HBSS into the right ventricle. When the color of the lungs changed to white, the lungs were excised avoiding the peritracheal lymph nodes. Lungs were then removed, washed in HBSS and cut into 3-mm pieces, and incubated in Iscove's Modified Dulbecco's Medium containing 1 mg/ml collagenase IV (Sigma) for 30 min at 37°C on a rotary agitator (approximately 60 rpm). Any remaining intact tissue was disrupted by passage through a 21-gauge needle. Tissue fragments and majority of the dead cells were removed by a 250-micrometer mesh screen, and cells were collected after centrifugation.

Ex Vivo Stimulation and Intracellular Cytokine Staining

Spleen and intraparenchymal lung lymphocytes from immunized and control animals were analyzed for protein S-specific CD8+ T cell responses. 1–1.5 × 10^6 cells were incubated for 20 h with 2 protein S peptide pools (S1 and S2, homologous to vaccine insert) (JPT Peptide Technologies, Berlin, Germany; PM-WCPV-S1). Peptide pools contain pools of 15-meric peptides overlapping by 11 amino acids covering the entire S protein (UniProt: P0DTC2) of SARS-CoV-2. Pool of 315 peptides (delivered in two subpools of 158 and 157 peptides) derived from a peptide scan through Spike glycoprotein. Peptide pools were combined (S1+S2) and used at a final concentration of 1.25 ug/ml of each peptide, followed by addition of Brefeldin A (BD GolgiPlug™; BD Biosciences, San Diego, CA, USA) (10 ug/ml) for the last 5 h of the incubation. Stimulation without peptides served as background control. The results were calculated as the total number of cytokine-positive cells with background subtracted. Peptide stimulated and non-stimulated cells were first labeled with live/dead detection kit (Thermo Fisher Scientific, Waltham, MA, USA) and then resuspended in BD Fc Block (clone 2.4G2) for 5 min at room temperature prior to staining with a surface-stain cocktail containing the following antibodies purchased from BioLegend® (San Diego, CA, USA): antigen presenting cell (APC)Cy7 CD45: Clone: 2D1; AF700 CD3: Clone: 17A2; APC CD4: Clone : RM4-5; PerCP CD8: Clone:53-6.7; PE Dazzle CD69: Clone:H1.2F3; BV 605 CD44: Clone : IM7; BV510 CD62L: Clone: MEL-14; PerCP/Cy5.5 CXCR6 (CD186): Clone: SA051D1. After 30 min, cells were washed with a flow cytometry staining buffer and then fixed and permeabilized using BD Cytofix/Perm fixation/permeabilization solution kit (according to manufacturer instructions), followed by intracellular staining using a cocktail of the following antibodies purchased from BioLegend: Alexa Fluor 488 interferon (IFN) gamma: Clone: XMG1.2; PE interleukin 2 [IL-2]: Clone: JES6-5H4 PE Cy7 tumor necrosis factor alpha (TNFα): Clone: MPG-XT22.

Data were collected on Spectral analyzer SONY SP6800 instrument (Sony Biotechnologies, Inc, San Jose, CA, USA). Analysis was performed using FlowJo™ software version 10.8 (Tree Star Inc, Ashland, OR, USA). Cells were first gated on live cells and then lymphocytes were gated for CD3+ and progressive gating on CD8+ T cell subsets. Antigen-responding CD8 (cytotoxic) T cells (IFNγ, or IL-2, or TNFα-producing/expressing cells) were determined either on the total CD8+ T cell population or on CD8+ CD69+ cells.

HLA-A2 Pentamer Staining

A total of 1–2 x 10^6 spleen, BAL, or lung cells were labelled with peptide-MHC class I (HLA 02-01) pentamer-APC (ProImmune, Oxford, UK) and incubated for 15 min at 37°C. Cells were labelled with LIVE/DEAD™ Fixable Violet—Dead Cell Stain Kit (Invitrogen, Carlsbad, CA, USA) and then stained with the following antibody cocktail: APCCy7 CD45: Clone:2D1; AF700 CD3: Clone: 17A2; PECy7 CD4: Clone : RM4-5; FITC CD8: Clone: KT15 (ProImmune, Oxford, UK) or PerCP CD8: Clone:53-6.7; PE Dazzle CD69: Clone:H1.2F3; BV 605 CD44: Clone : IM7; BV510 CD62L: Clone: MEL-14; PerCP/Cy5.5 CXCR6: Clone: SA051D1. Spleen and lung cells that were stimulated overnight with peptide pools (as described under

ex vivo stimulation and intracellular staining) were fixed and permeabilized with Cytofix/Perm solution (BD) and then stained for intracellular cytokines: IFNγ, and IL-2. Cells were acquired on SP6800 Sony instrument and data analyzed using FlowJo software version 10.8. Data were analyzed using forward side-scatter single-cell gate followed by CD45, CD3, and CD8 gating, then pentamer gating within CD8+ T cells. These cells were then analyzed for expression of markers using unstained and overall CD8+ population to determine the placement of the gate. Single-color samples were run for compensation and fluorescence minus 1 control sample were also applied to determine positive and negative populations, as well as channel spillover.

STATISTICS

All experiments were conducted independently at least 3 times on different days. Comparisons of flow cytometry cell frequencies were measured by the 2-way analysis of variance (ANOVA) test with Holm-Sidak multiple-comparison test, *p<0.05, **p<0.01, and ***p<0.001, or unpaired T-tests (2-tailed) were carried out to compare the control group with each of the experimental groups (alpha level of 0.05) using the Prism software (GraphPad Software, San Diego, CA, USA). Welch's correction was applied with the unpaired T test, when the p-value of the F test to compare variances were ≤0.05. Data approximately conformed to Shapiro-Wilk test and Kolmogorov-Smirnov tests for normality at 0.05 alpha level. Data were presented as mean ± standard deviation in the text and in the figures. All statistical analysis was conducted using GraphPad Prism 8 software.

RESULTS

AD100 and HEK-293 Express gp96-Ig and Protein S

Cell-based secreted heat shock protein technology has been previously validated in numerous animal models and in humans (37–39, 42). The secreted form of gp96 protein (gp96-Ig) was generated by replacing the c-terminal, KDEL-retention sequence of human gp96 gene, with hinge region and constant heavy chains (CH2 and CH3) of human IgG1 (43) (**Figure 1A**). The pcDNA 3.1(–) vector was used to express SARS-CoV-2 spike (S) protein (in this manuscript referred as protein S) (**Figure 1A**), due to its propensity to constitutively express large amounts of the protein in mammalian cells. Complementary (c) DNA encoding the full-length SARS-CoV-S glycoprotein included Kozak sequence (GCCACC) to optimize expression in eukaryotic cells and the open-reading frame contained endogenous leader sequence, transmembrane, and cytosolic domains.

Vaccine cells, 293-gp96-Ig-S and AD100-gp96-Ig-S, were generated by cotransfection of AD100 and HEK293 cells with plasmids encoding gp96-Ig (B45) and protein S (pcDNA 3.1) and selection with G418 and L-histidinol as described in *Methods*. We confirmed by ELISA that both stable transfected cell lines secreted gp96-Ig into culture supernatants at a rate of 125 ng/ml/24 h/10^6 vaccine cells (**Figure 1B**). Our previous data indicate that gp96-Ig accumulation in cell culture supernatant is linear and time dependent (35, 43).

Protein S expression by the vaccine cells was confirmed by analyzing vaccine cell lysates on SDS page, blotting with anti-SARS-CoV-2 S antibody (**Figure 1C**) and by immunofluorescence (**Figure 1D**). We observed expression of full-length protein S (250 kDa) only in AD100 transfected cell lines (lanes 2–4) but not in nontransfected AD100 cell line (lane 1). In addition, we observed molecular weight bands of 120 and 130 kDa that could represent cleavage products of full length protein S (protein S1 and S2) and/or gp96-Ig fusion protein chaperoning the protein S peptides. The expected molecular weight of gp96-Ig fusion protein is 116 kDa. Additional bands, of ~70 kDa, were found to be expressed only in the transfected cell line and were not observed in the nontransfected AD100 cells. However, nonspecific bands of 100, 60, and 40 kDa were observed in the AD100 parental cell line. Recombinant protein S1 130 kDa was used as a positive control. We calculated the ratio of protein S to β-actin expression (**Figure 1C**) and confirmed the expression of protein S by immunofluorescence (**Figure 1D**). We observed cytoplasmic and transmembrane distribution of protein S in AD100-gp96-Ig-S cell line. We therefore confirmed the expression of gp96-Ig and S protein in our AD100 cell line and used it for immunogenicity studies as described below.

Secreted gp96-Ig-S Vaccine Induces CD8+ T Cell Effector Memory Responses in the Lungs

Our vaccination strategy is based on the quantity of gp96-Ig-S secreted by the vaccine cells to stimulate CD8+ CTL responses *via* APC cross-presentation. The vaccination dose, is therefore, standardized to a set amount of gp96-Ig secreted by 10^6 vaccine cells within 24 h. It has been well established from our previous vaccine immunogenicity studies that the optimal dose for induction of CD8+ T cell specific responses in mice is 200–500 ng/ml (33, 35, 38, 39, 43). Here, we used 200 ng/ml to immunize mice with AD100-gp96-Ig-S vaccine. Mice were vaccinated *via* the s.c. route and, after 5 days, the frequency of T cells within spleen, lungs (lung parenchyma), and BAL cells (lung airways) was determined. We observed significant increase in the frequencies of CD8+ T cells in the spleen and lungs, but not within the BAL of vaccinated mice (**Figure 2A**). Frequency of CD4+ T cells was unchanged between vaccinated and control mice in all analyzed tissues. It is well established that vaccination with gp96-Ig induces CD8+ TEM differentiation (33, 37, 39). Here, we confirmed that gp96-Ig-S vaccine primes strong effector memory CD8+ T-cell responses as determined by analysis of CD44 and CD62L expression (**Figure 2B**). Whereas the frequency of naïve (N), CD44-CD62L+CD8 T cells and central memory (CM), CD44+CD62L+ CD8+ T cells was unchanged, we found statistically significant increase of TEM CD44+ CD62L- CD8+ T cells within the spleen and lungs (**Figure 2B**). In addition, we observed a trend of more TEM CD8+

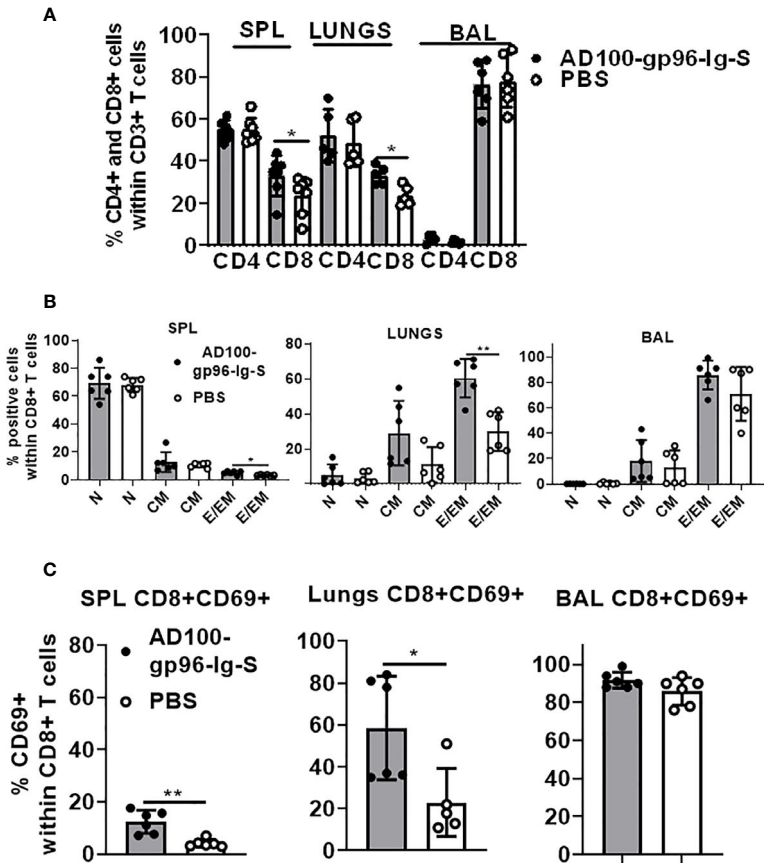

FIGURE 2 | Secreted gp96-Ig-S vaccine induces CD8+ TEM and TRM responses in the lungs. Equivalent number of AD100-gp96-Ig-S vaccine cells that produce 200 ng/ml gp96-Ig or PBS were injected by s.c. route in C56Bl/6 mice. 5 days later, mice were sacrificed and spleen, lungs, and BAL were isolated and **(A)** frequency of CD4+ and CD8+ T cells; **(B)** naive (N) CD44-CD62L+, CM CD44+CD62L+ and EM CD44+CD62L- CD8+ T cells; and **(C)** TRM CD69+ cells were determined by flow cytometry after staining the cells with antibodies against the following surface markers: CD45, CD3, CD4, CD8, CD44, CD62L, and CD69 antibodies. Bar graph shows percentage of CD4+ and CD8+ cells within CD3+ cells or CD8+ T cell memory subset within CD8+ T cells. Data represent at least two technical replicates with three to six independent biological replicates per group. *p<0.05, **p<0.01. **(A, B)** Mann-Whitney tests were used to compare two experimental groups. To compare >2 experimental groups, Kruskal-Wallis ANOVA with Dunn's multiple comparison tests were applied). BAL, bronchoalveolar lavage; CM, central memory; EM, effector memory; TEM, T cell effector memory.

T cells within the CD8+ T cells in the BAL (**Figure 2B**). TRM cells are a distinct memory T cell subset compared to CM and EM cells (44) that are uniquely situated in different tissues, including lungs (30, 31). One of the canonical markers of TRM T cells is CD69 (20, 44, 45). We found that there was a significant increase in the frequency of CD8+CD69+ T cells in vaccinated mice compared to control, non-vaccinated mice in both spleen and lungs (**Figure 2C**). Even though the frequency of CD8 +CD69+ T cells was the highest in the BAL compared to spleen and lungs, we did not observe a difference in their frequencies between vaccinated and control mice. Overall, vaccination with AD100-gp96-Ig-S induced robust TEM and CD69+ CD8+ T cell responses in both spleen and lungs. Our vaccine can therefore successfully elicit both systemic and tissue-specific immune response, which is pivotal in conferring robust immunity against infection such as against SARS-CoV-2.

Both Protein S-Specific CD8+ and CD4+ T Helper 1 T Cell Responses Are Induced by gp96-Ig-S Vaccine

To evaluate polyepitope, protein S-specific CD8+ and CD4+ T-cell responses induced by gp96-Ig-S vaccination, we used pooled S peptides (S1+S2) and a multiparameter intracellular cytokine-staining assay to assess Th1 (IFNγ+, IL-2+, and TNFα+), CD8+ and CD4+ T cells (**Figure 3**). Spleen and lung cells were tested for responses to the pool of overlapping protein S peptides (S1 + S2) and all of the vaccinated animals showed significantly higher magnitude of the protein S-specific T cell responses against S1 and S2 epitopes compared with non-vaccinated controls (**Figures 3A–E**). Increase in the vaccine-induced Th1 CD8+ T cell responses (IFNγ+, IL-2+, and TNFα+) was noted in both spleen and lungs (**Figures 1A, B**), whereas Th1 CD4+ T cell responses (IFNγ+, IL-2+, and TNFα+) were induced only in lungs (**Figures 3C, D**). The proportion of the protein S-specific CD8+ T cells that produce

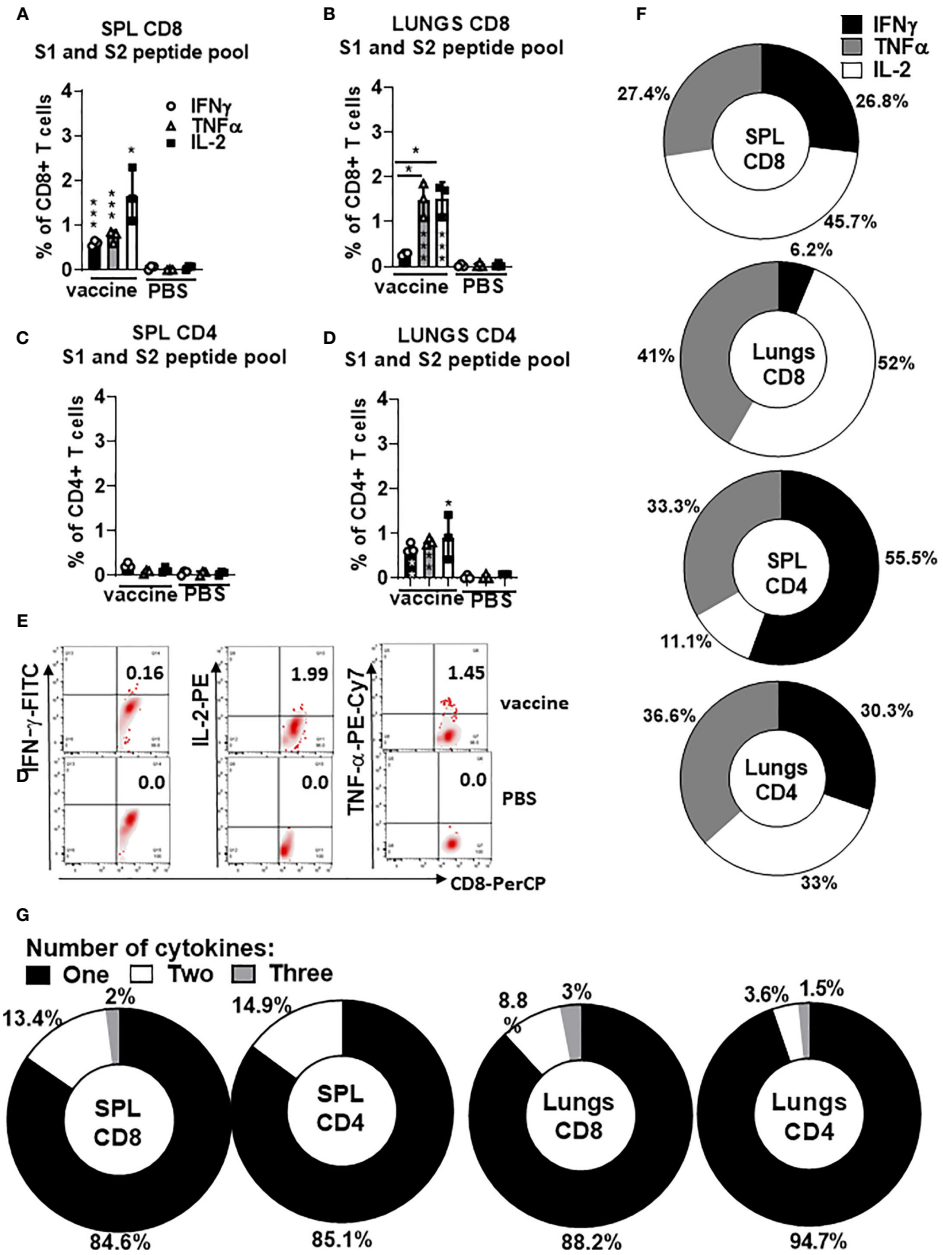

FIGURE 3 | Secreted gp96-Ig-S vaccine induces protein S specific CD8+ and CD4+ T cells in the spleen and lung tissue. Five days after the vaccination of C57Bl6 mice, splenocytes and lung cells were isolated from vaccinated and control mice (PBS) and in vitro restimulated with S1 and S2 overlapping peptides from SARS-CoV-2 protein in the presence of protein transport inhibitor, brefeldin A for the last 5 h of culture. After 20 h of culture, ICS was performed to quantify protein S-specific CD8+ and CD4+ T-cell responses. Cytokine expression in the presence of no peptides was considered background and it was subtracted from the responses measured from peptide pool stimulated samples for each individual mouse. **(A, B)** CD8+ T cells from spleen and lungs expressing IFNγ, TNFα, and IL-2 in response to S1 and S2 peptide pool; **(C, D)** CD4+ T cells from spleen and lungs expressing IFNγ, TNFα, and IL-2 in response to S1 and S2 peptide pool; **(E)** Representative dot plot of gated CD8+ T cells in lungs expressing indicated cytokines (IFNγ, IL-2, and TNFα) in vaccinated and non-vaccinated (PBS, control) HLA-A2 mice at day 5 **(F)** Proportion of antigen (protein S)-experienced CD8+ and CD4+ T cells isolated from spleen and lung tissue expressing IFNγ, TNFα, or IL-2 after o/n stimulation with S1 + S2 peptides. Pie charts corresponding to cytokine profiles of CD8+ and CD4+ T cells isolated from spleen and lung tissue; **(G)** Pie charts corresponding to cytokine profiles of CD8+ CD4+ T cells isolated from spleen and lung tissue after o/n stimulation with S1 + S2 peptides. Assessment of the mean proportion of cells making any combination of one to three cytokines (IFN-γ, TNFα, IL-2). Data represent at least two technical replicates with three to six independent biologic replicates per group. *p<0.05, ***p<0.001. Kruskal-Wallis ANOVA with Dunn's multiple comparisons tests were applied. Asterisks (*) above or inside the column denote significant differences between indicated T cells producing cytokines in vaccine versus control (PBS) at 0.05 alpha level. ANOVA, analysis of variance; ICS, intracellular cytokine staining; IFN, interferon; IL, interleukin; PBS, phosphate-buffered saline; TNF, tumor necrosis factor.

IFNγ (26.8%) was significantly reduced in the lungs (6.2%), while both TNFα and IL-2 productions were increased in the lungs (41% and 52%, respectively) compared to spleen (27.4% and 45.7%, respectively) (**Figure 3F**). We found that the proportion of the protein S-specific CD4+ T cells that produce IFNγ was higher in the spleen than in the lungs [55.5% (spleen) versus 30.3% (lungs)], whereas IL-2 production was higher in the lungs than in the spleen [33% (lungs) versus 11.1% (spleen)] (**Figure 3F**). Further assessment of protein S-specific CD8+ and CD4+ T cells in the spleen and lungs revealed that the vast majority of protein S-specific CD8+ and CD4+ T cells, irrespective of their location, synthesized only 1 cytokine (**Figure 3G**).

It was therefore confirmed that a polyepitope, S-specific, CD4+, and CD8+ T cell response was generated in the spleen and lungs to different extents, providing a strong vaccine-induced Th1 cellular immune responses.

Induction of SARS-CoV-2 Protein S Immunodominant Epitope-Specific CD8+ T Cells in the Lungs and Airways of Vaccinated HLA-A2.1-Transgenic Mice

Recently, it was reported that SARS-CoV-2-specific memory CD8+ T cell responses generated against cognate antigens positively correlate with a number of symptom-free days after infection (14, 16). Therefore, it is important to develop vaccines that can elicit SARS-CoV-2-specific CD8+ T cells. Having identified overall T-cell responses to SARS-CoV-2 protein S (**Figure 3**), we wanted to determine whether gp96-Ig-S vaccine induced HLA class I-specific cross-presentation of immunodominant SARS-CoV-2 protein S epitopes. In order to do this, we used transgenic HLA-A2.1 mice and HLA class I pentamers as probes to detect CD8+ T cells specific for two immunodominant SARS-CoV-2 protein S epitopes: YLQPRTFLL (YLQ) (aa 269-277) and FIAGLIAIV (FIA) (aa 1220-1228) in vaccinated mice (**Figures 4A–C**). We found that the vaccine effectively induces both YLQ+CD8+ T cells, as well as FIA+CD8+ T cells in the spleen, lungs, and BAL (**Figures 4A–C**). Interestingly, we found the highest frequency of YLQ+CD8+ T cells in the BAL of vaccinated mice and the lowest frequency of YLQ+ and FIA+ CD8+ T cells was observed in the lungs 5 days after primary vaccination. Importantly, we observed that after contraction of vaccine induced YLQ+CD8+ and FIA+CD8+ T cell responses in spleen, lungs and BAL, frequency of S-specific CD8+ T cell responses is preserved and it is significantly higher in BAL compared to non-vaccinated controls (**Figures 4A–C**).

Upon further phenotype analysis of YLQ+CD8+ T cells, it was confirmed that they express both CD69 and CXCR6 (**Figure 4D**). Particularly, we found that during primary response (day 5) all YLQ+CD8+ T cells in the BAL were also CD69+ and CXCR6+, and the frequency of YLQ+CD8+CXCR6+ cells was significantly higher in the BAL compared to the lungs. However, during contraction phase (day 30) YLQ+CD8+ cells (**Figures 4A, B** and **Supplementary Figure 1**) in the SPL, lungs and BAL express both, CD69 and CXCR6 (**Figure 4D**).

We confirmed that S-specific CD8+ and CD4+ T cells are present in significantly higher frequencies compared to unvaccinated controls 30 days after single dose vaccination (**Figures 5A–E**). The proportion of the protein S-specific CD8+ T cells that produce IFNγ was comparable in the spleen and lungs (32.7% and 28%, respectively) while we observed increased proportion of the cells that produce TNFα in the lungs (47.3%) compared to spleen (24.5%) (**Figure 5C**). In addition, we found that the proportion of the protein S-specific CD8+ T cells that produce IL-2 was higher in the spleen than in the lungs (42.6% and 24.5%, respectively) while the proportion of S-specific CD4+ T cells that produce IL-2 was higher in lungs than in spleen (44.4% and 33.3%, respectively) (**Figure 5C**).

Furthermore, we observed increase in the frequency of YLQ+ CD8+ T cells in the spleen, lungs and BAL in all animals after receiving second dose of gp96-S vaccine at day 30 (**Figure 5F**). Despite the similar magnitudes of primary and secondary CD8+ T cell expansion, contraction of vaccine induced Ag-specific CD8+ T cell responses was different during primary and secondary response. We observed more rapid contraction of CD8+ T cells after primary vaccination, with 68% loss of Ag-specific CD8+ T cells from day 5 to 30 (**Figure 5G**), compared to 25% decrease in Ag-specific CD8+ T cells during secondary response (**Figure 5G**). Thus, the program of contraction in CD8+ T cells that are responding to second dose of vaccine was prolonged, resulting in increased frequencies of memory S-specific CD8+ T cells.

DISCUSSION

Our vaccine approach is based on the gp96-Ig platform technology that elicits potent, antigen-specific CD8+ T-cells. This proprietary secreted heat shock protein platform has been successfully used to induce immunogenicity against tumors, HIV/SIV, Zika, and malaria in different animal models (37–39, 46–48). Importantly, this vaccine strategy has shown success in delaying virus acquisition, as well as in improving the survival of NSCLC patients in clinical trials (38, 42).

The principle of a cell-based vaccine relies on the ability of gp96-Ig to chaperone antigenic proteins to be efficiently endocytosed and cross-presented by activated dendritic cells (DC) to CD8+ T cells, thereby stimulating an avid, pathogen-specific T-cell response (33, 34, 37–39). We adapted this cell-based technology to create a vaccine that delivers SARS-CoV-2 spike (S) protein directly to DCs, so that primed and activated SARS-CoV-2 protein S-specific CD8+ T cells can identify and kill SARS-CoV-2 infected lung epithelial cells. We generated vaccine cells by co-expressing secreted gp96-Ig and full-length protein S. Gp96-Ig is an endoplasmic reticulum chaperone that, together with TAP (transporter associated with antigen processing) and calreticulin in the endoplasmic reticulum, is thought to constitute a relay line for antigenic peptide transfer from the cytosol to MHC class I molecules in a concerted and regulated manner (49, 50). The gp96-antigenic peptide complexes are predominantly internalized by subsets of APCs through cell surface receptor CD91. Internalized gp96 can effectively present the associated peptides to MHC class I and II molecules and thus activate specific CD8+ and CD4+ T-cell responses (34, 39, 51, 52). We expressed full-length protein

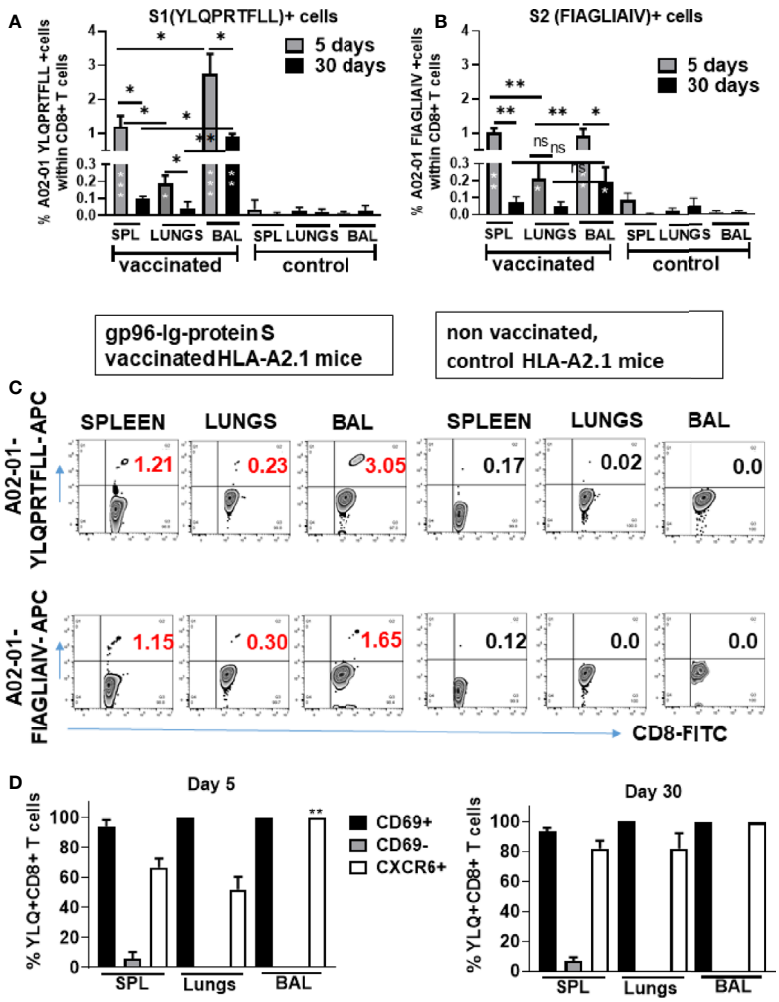

FIGURE 4 | Secreted Gp96-Ig-S vaccine induces S1- and S2-specific CD8 + CD69 + CXCR6 + cells in the spleen, lung tissue, and BAL. Five and 30 days after the vaccination of HLA-A2.1 transgenic mice, splenocytes, lung cells and BAL were isolated form vaccinated and control mice (PBS). Cells were stained with HLA-A2 pentamer containing FIAGLIAIV and YLQPRTFLL peptides, followed by surface staining for CD45, CD3, CD4, CD8, CD69, CXCR6. **(A, B)** Bar graphs represent percentage of the pentamer positive cells within CD8+ T cells; **(C)** Representative zebra plots of gated CD8+ T cells expressing indicated pentamer-specific TCR+ CD8+ T cells in vaccinated and non-vaccinated HLA-A2.1 mice at day 5 **(D)** Bar graphs represent percentage of CD69+, CD69-, and CXCR6+ cells within YQL-pentamer positive cells at days 5 and 30; (Data represent at least two technical replicates with three to six independent biologic replicates per group. *p<0.05, **p<0.01, ***p<0.001. Kruskal-Wallis ANOVA with Dunn's multiple comparisons tests were applied. Asterisks (*) inside the column denote significant differences between indicated pentamer+CD8+ T cells in the vaccinated group and control (PBS) **(A, B)** at 0.05 alpha level. ANOVA, analysis of variance; BAL, bronchoalveolar lavage; PBS, phosphate-buffered saline.

S in the vaccine cells to ensure broad representation of all immunodominant protein S peptides (S1- and S2-derived peptides) by secreted gp96-Ig. Since coronaviruses assemble in the compartment between the endoplasmic reticulum and Golgi apparatus (53, 54) and the S leader directs it to the endoplasmic reticulum, the native leader sequence of protein S was retained, as well as transmembrane and cytosolic domain. We confirmed in previous studies that secreted gp96-Ig provides immunologic specificity for the antigenic repertoire expressed inside the cells, including surrogate antigen ovalbumin, as well as numerous tumor or infectious antigens, but does not cross-immunize to different cell-derived antigens (35, 37–39). Our data are consistent with the explanation that S1 and S2 peptides associated with secreted gp96-Ig are transferred to and presented by class I and II MHC and stimulate a S1- and S2-specific CD8+ and CD4+ T cell response. We confirmed that vaccination with AD100-gp96-Ig-S induces CD8+ T cells specific for S1- and S2-immunodominant epitopes in both lungs and airways. Most importantly, this is a proof-of-concept study that will be applied to other structural proteins such as nucleocapsid protein, membrane protein, and nonstructural proteins such as NSP-7, NSP-13 of ORF-1 that all have been reported to be important in induction of SARS-CoV-2-specific CD4+ and CD8+ T cell responses in convalescents (7, 10, 11, 55).

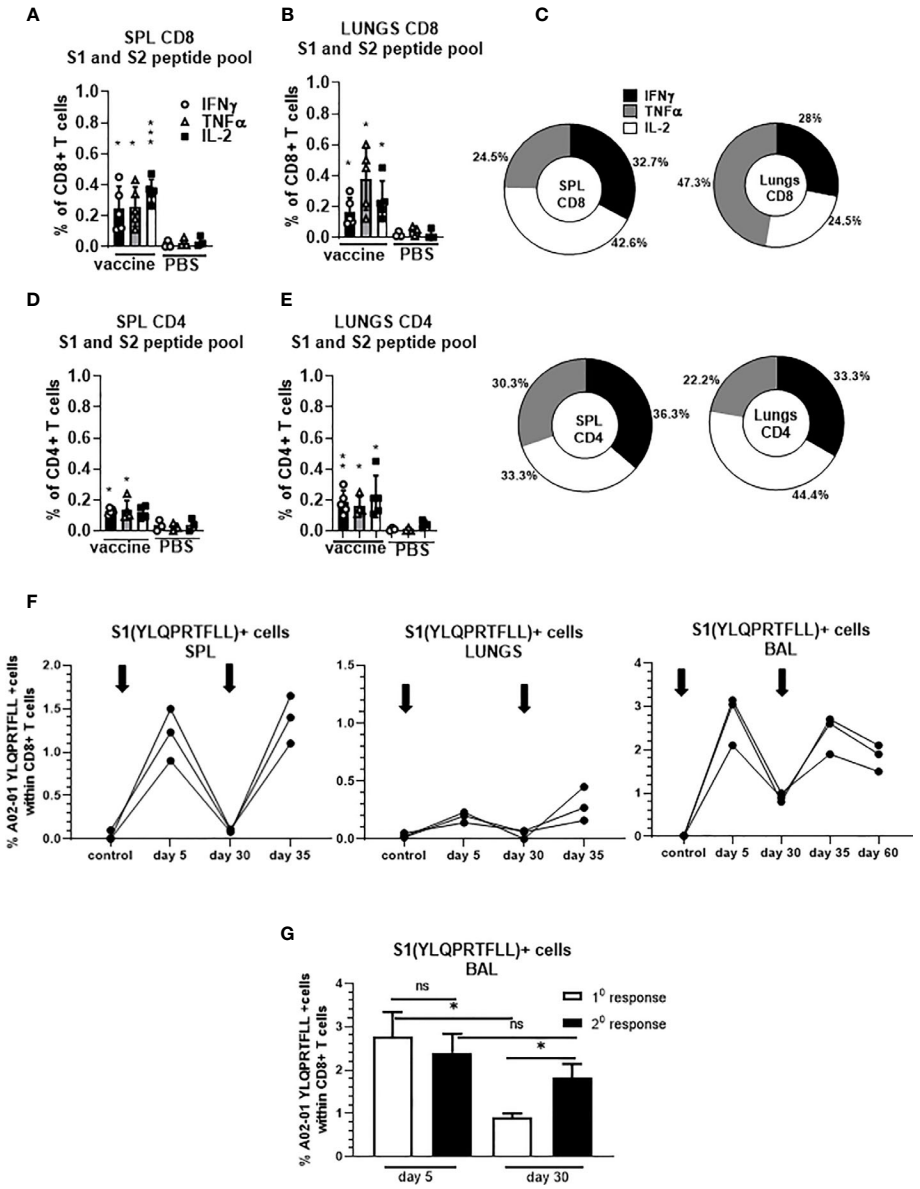

FIGURE 5 | Secreted gp96-Ig-S vaccine induces protein S specific memory CD8+ and CD4+ T cells in the spleen and lungs. Thirty days after the vaccination of HLA-A2.1 transgenic mice, splenocytes and lung cells were isolated from vaccinated and control mice (PBS) and in vitro restimulated with S1 and S2 overlapping peptides from SARS-CoV-2 protein in the presence of protein transport inhibitor, brefeldin A for the last 5 h of culture. After 20 h of culture, ICS was performed to quantify protein S-specific CD8+ and CD4+ T-cell responses. Cytokine expression in the presence of no peptides was considered background and it was subtracted from the responses measured from peptide pool stimulated samples for each individual mouse. **(A, B)** CD8+ T cells from spleen and lungs expressing IFNγ, TNFα, and IL-2 in response to S1 and S2 peptide pool; **(D, E)** CD4+ T cells from spleen and lungs expressing IFNγ, TNFα, and IL-2 in response to S1 and S2 peptide pool; **(C)** Proportion of antigen (protein S)-experienced CD8+ and CD4+ T cells isolated from spleen and lung tissue expressing IFNγ, TNFα, or IL-2 after o/n stimulation with S1 + S2 peptides. Pie charts corresponding to cytokine profiles of CD8+ and CD4+ T cells isolated from spleen and lung tissue; **(F)** 5 days after primary and secondary vaccination of HLA-A2.1 transgenic mice, splenocytes, lung cells and BAL were isolated form vaccinated and control mice (PBS). Time of primary and secondary vaccination is indicated with black arrows. Cells were stained with HLA-A2 pentamer containing YLQPRTFLL peptide, followed by surface staining for CD45, CD3, CD4, CD8. **(G)** BAL was analyzed 5 and 30 days after primary and secondary vaccination and frequency of HLA-A2 pentamer positive cells was determined. Graphs represent percentage of the pentamer positive cells within CD8+ T cells in individual mice; Data represent at least two technical replicates with three to six independent biologic replicates per group. *p<0.05, **p<0.01, ***p<0.001, ns, not significant. Kruskal-Wallis ANOVA with Dunn's multiple comparisons tests were applied. Asterisks (*) above or inside the column denote significant differences between indicated T cells producing cytokines in vaccine versus control (PBS) at 0.05 alpha level. ANOVA, analysis of variance; ICS, intracellular cytokine staining; IFN, interferon; IL, interleukin; PBS, phosphate-buffered saline; TNF, tumor necrosis factor.

In agreement with our previous findings (33, 38, 39), the gp96-Ig vaccine resulted in the preferential induction of CD8+ T cell responses systemically and in epithelial compartments. However, this is the first report about the increase in the frequencies of vaccine induced CD8+ T cells in the lungs (**Figure 1A**). TEM CD8+ T cells are considered to constitute the frontline defense within the different epithelial compartments including lungs and airways, which promptly recognize and kill infected cells. Our data suggest that after a single dose of AD100-gp96-Ig-S immunization there is preferential compartmentalization of TEM and TCM immune responses in the lungs and BAL compared to the spleen where a majority of cells are naïve CD8+ T cells (**Figure 1B**). However, additional memory cells without migratory potential such as TRM CD8+ T cells, exist within the tissues including lungs and airways (20, 44, 45, 56). Since TRM are uniquely situated in the lungs to immediately respond to reinfection, by inducing the protein-S-specific CD8+ T cells that home to the lungs, gp96-Ig-S vaccine provides an ideally balanced generation of both arms, TRM and TEM, of the memory response in the lungs. To further gauge the effect of gp96-Ig vaccination on the induction of epitope specific immunogenicity, we used pentamers to detect S1 and S2 epitope-specific CD8+ T cell responses. We found that gp96-Ig induced the highest frequencies of S1- and S2- epitope specific CD8+ T cells in the airways. In light of the new findings about exclusive highly clonally expanded SARS-CoV-2-specific CD8+ T cells with preferentially expressed tissue-resident genes (XCL1, CXCR6, and ITGAE) in the BAL of moderate COVID-19 cases (57) and not in the critical/severe COVID-19 patients, induction of SARS-CoV-2 specific CD8+ T cells that home to airway epithelium emphasizes the importance of developing vaccination strategies that induce TRM antigen-specific CD8+ T cells that will improve efficacy of vaccination against respiratory pathogens including SARS-CoV-2.

It is well appreciated that the antigen presenting cells at the site of immunization direct the imprinting of the ensuing T-cell response and control the expression of trafficking molecules (58). Priming of CD8+ T cells by CD103+ DC was found to promote TRM CD8+ T cell differentiation and migration into peripheral epithelial tissues, including lungs (56, 59). Our previous studies indicated that gp96-Ig immunization increases frequency of $CD11c^{high}$ MHC class II^{high} CD103+ cells at the vaccination site (33). In light of our previous findings and findings of Bedoui et al. (60) that CD103+ DCs are the main migratory subtype with dominant cross-presenting ability, induction of CD103+ DCs by gp96 represents an ideal vaccination strategy for priming effective and durable immunity in the epithelial tissues. We also hypothesize that secretory gp96-Ig can be captured by lung DC upon s.c. inoculation and in that way directly induce tissue memory responses and even more importantly support their longevity in the tissue. It was previously shown that, based on differences in the localization and functions, there are two different subsets of lung TRM cells: airway TRM and interstitial TRM (61–63). CXCR6-CXCL16 interactions are crucial in controlling the localization of virus-specific TRM CD8+ T cells in the lungs and maintaining the airway TRM cell pool (20). Moreover, blocking of CXCR6-CXCL16 interactions significantly decreases the steady-state migration of TRM cells into airways, so vaccine induced SARS-CoV-2 S specific CD8+ T cells that express CXCR6 fulfill one of the major requirements for continued CXCR6 signaling in maintaining the airway TRM pool (20). *In vivo* anti-CD3 labelling of the lymphocytes is the best method for distinguishing intravascular vs extravascular antigen specific cells. Future studies should include *in vivo* labelling to distinguish if vaccine induced S-specific immune responses are circulating/effector or local/tissue resident cells.

We have confirmed in different infectious vaccine models that gp96-Ig carries all peptides of a cell that are selected in the recipient/vaccinee for MHC I, having the broadest, theoretically possible antigenic epitope-spectrum for cross-priming of CD8+ T cells by any MHC I type. Here, we showed that AD100-gp96-Ig-S resulted in the polyepitope and polyfunctional protein S-specific CD8+ and CD4+ T cell responses (**Figure 3**). When stimulated *in vitro* with S1+S2 peptides, spleen and lung CD8+ T cells produce IFNγ, TNFα, and IL-2 cytokines (**Figure 3**) with CD8+ T cells in the lungs producing significantly less IFNγ than the CD8+ T cells in the spleen. It is known that enhanced activation, resulting from high levels of inflammation, induces CD8+ T cells entering the lungs to produce regulatory cytokines (64) that initiate "dampening" of the immune response in order to prevent any excessive damage of the lung tissue. In addition, we report that CD4+ T cells in the lungs produce all 3 Th1 cytokines in equal ratio (**Figure 3F**). This finding is in line with our previous report discussing gp96-Ig induced SIV-specific CD4+ T cells in the lamina propria which were almost the exclusive producers of IL-2 (33). Further studies will therefore be required to evaluate the role of protein-S specific CD4+ T cells in the induction of B cell and antibody responses. Previously, we have shown that gp96 is a powerful Th1 adjuvant for CTL priming and for stimulation of Th1 type antibodies in mice and nonhuman primates (37, 38). In addition, we will evaluate memory responses after a single and booster dose to establish the best vaccination protocol for future challenge studies.

In summary, we provide a paradigm for a novel vaccine development approach capable of induction of cellular immune responses in epithelial tissues such as the lungs. Structure-guided SARS-CoV-2 S protein combined with a safe and efficacious gp96-Ig vaccine platform can pave the way for a protective and durable immune response against COVID-19. This is a first demonstration of the utility and versatility of our proprietary secreted gp96-Ig SARS-CoV-2 vaccine platform that can be rapidly engineered and customized based on other and future pathogen sequences. Furthermore, the platform is proof of concept for the prototype vaccine approach for similar pathogens that require induction of effective TRM responses in epithelial tissues.

DATA AVAILABILITY STATEMENT

The raw data supporting the conclusions of this article will be made available by the authors, without undue reservation.

ETHICS STATEMENT

The animal study was reviewed and approved by University of Miami Institutional Animal Care & Use Committee.

AUTHOR CONTRIBUTIONS

NS conceived and coordinated the experiments and obtained funding. EF, LP, KP, KO'N, and NS performed the experiments and analyzed the data. MS provided reagents. NS, EF, PJ, RJ, and MS wrote the paper. All authors contributed to the article and approved the submitted version.

FUNDING

This work was supported by Heat Biologics, Inc (AWD-005840) (NS) and by Department of Microbiology and Immunology (NS) and University of Miami (NS).

ACKNOWLEDGMENTS

This manuscript has been released as a pre-print at *bioRxiv* (65). We dedicate this work to the late Dr. Eckhard Podack. We are grateful to all members of Strbo laboratory, Heat Biologics, Inc. CEO Jeff Wolf, Chief Scientific and Operating Officer, Jeff Hutchins, and Director Discovery Sciences, Eric Dixon, for their overall support, advice, and editorial contributions. We are grateful to Mr. William Strong for his generous gift for vaccine development. We thank Sylvester Comprehensive Cancer Center Flow Cytometry Shared Resource (SCCC FCSR) staff for their help.

SUPPLEMENTARY MATERIAL

The Supplementary Material for this article can be found online at: https://www.frontiersin.org/articles/10.3389/fimmu.2020.602254/full#supplementary-material

SUPPLEMENTARY FIGURE 1 | Secreted Gp96-Ig-S vaccine induces S1-specific CD8 + cells in the spleen, lung tissue, and BAL. Thirty days after the vaccination of HLA-A2 transgenic mice, splenocytes, and lung cells and BAL were isolated from vaccinated and control mice (PBS). Cells were stained with HLA-A2 02-01 pentamer containing SARS-CoV2 YLQPRTFLL peptide, followed by surface staining for CD45, CD3, CD4, CD8, CD69, CXCR6. Representative zebra plots of gated CD8+ T cells expressing indicated pentamer-specific TCR+ CD8+ T cells in vaccinated and non-vaccinated HLA-A2 mice at day 30. HLA-A2 pentamer containing HIV/SIV (HIV-1 gag) SLYNTVATL pentamer was used as a negative control pentamer.

REFERENCES

1. Du L, He Y, Zhou Y, Liu S, Zheng BJ, Jiang S. The spike protein of SARS-CoV–a target for vaccine and therapeutic development. *Nat Rev Microbiol* (2009) 7(3):226–36. doi: 10.1038/nrmicro2090
2. Watanabe Y, Berndsen ZT, Raghwani J, Seabright GE, Allen JD, Pybus OG, et al. Vulnerabilities in coronavirus glycan shields despite extensive glycosylation. *Nat Commun* (2020) 11(1):2688. doi: 10.1038/s41467-020-16567-0
3. Ibarrondo FJ, Fulcher JA, Goodman-Meza D, Elliott J, Hofmann C, Hausner MA, et al. Rapid decay of anti–SARS-CoV-2 antibodies in persons with mild Covid-19. *N Engl J Med* (2020) 383(11):1085–7. doi: 10.1056/NEJMc2025179
4. Long QX, Tang XJ, Shi QL, Li Q, Deng HJ, Yuan J, et al. Clinical and immunological assessment of asymptomatic SARS-CoV-2 infections. *Nat Med* (2020) 26(8):1200–4. doi: 10.1038/s41591-020-0965-6
5. Channappanavar R, Fett C, Zhao J, Meyerholz DK, Perlman S. Virus-specific memory CD8 T cells provide substantial protection from lethal severe acute respiratory syndrome coronavirus infection. *J Virol* (2014) 88(19):11034–44. doi: 10.1128/JVI.01505-14
6. Tang F, Quan Y, Xin ZT, Wrammert J, Ma MJ, Lv H, et al. Lack of peripheral memory B cell responses in recovered patients with severe acute respiratory syndrome: a six-year follow-up study. *J Immunol* (2011) 186(12):7264–8. doi: 10.4049/jimmunol.0903490
7. Le Bert N, Tan AT, Kunasegaran K, Tham CYL, Hafezi M, Chia A, et al. SARS-CoV-2-specific T cell immunity in cases of COVID-19 and SARS, and uninfected controls. *Nature* (2020) 584(7821):457–62. doi: 10.1038/s41586-020-2550-z
8. Ferretti AP, Kula T, Wang Y, Nguyen DMV, Weinheimer A, Dunlap GS, et al. COVID-19 Patients Form Memory CD8+ T Cells that Recognize a Small Set of Shared Immunodominant Epitopes in SARS-CoV-2. *medRxiv* (2020) 07.24.20161653. doi: 10.2139/ssrn.3669387
9. Zhu N, Zhang D, Wang W, Li X, Yang B, Song J, et al. A Novel Coronavirus from Patients with Pneumonia in China, 2019. *New Engl J Med* (2020) 382 (8):727–33. doi: 10.1056/NEJMoa2001017
10. Grifoni A, Weiskopf D, Ramirez SII, Mateus J, Dan JM, Moderbacher CR, et al. Targets of T Cell Responses to SARS-CoV-2 Coronavirus in Humans with COVID-19 Disease and Unexposed Individuals. *Cell* (2020) 181 (7):1489–1501.e15. doi: 10.1016/j.cell.2020.05.015
11. Li CK, Wu H, Yan H, Ma S, Wang L, Zhang M, et al. T cell responses to whole SARS coronavirus in humans. *J Immunol* (2008) 181(8):5490–500. doi: 10.4049/jimmunol.181.8.5490
12. Zhao J, Zhao J, Perlman S. T cell responses are required for protection from clinical disease and for virus clearance in severe acute respiratory syndrome coronavirus-infected mice. *J Virol* (2010) 84(18):9318–25. doi: 10.1128/JVI.01049-10
13. Liu WJ, Lan J, Liu K, Deng Y, Yao Y, Wu S, et al. Protective T Cell Responses Featured by Concordant Recognition of Middle East Respiratory Syndrome Coronavirus-Derived CD8+ T Cell Epitopes and Host MHC. *J Immunol* (2017) 198(2):873–82. doi: 10.4049/jimmunol.1601542
14. Peng Y, Mentzer AJ, Liu G, Yao X, Yin Z, Dong D, et al. Broad and strong memory CD4 (+) and CD8 (+) T cells induced by SARS-CoV-2 in UK convalescent COVID-19 patients. *bioRxiv* (2020) 2020:06.05.134551. doi: 10.1101/2020.06.05.134551
15. Altmann DM, Boyton RJ. SARS-CoV-2 T cell immunity: Specificity, function, durability, and role in protection. *Sci Immunol* (2020) 5(54):eabf3698. doi: 10.1126/sciimmunol.abd6160
16. Sekine T, Perez-Potti A, Rivera-Ballesteros O, Strålin K, Gorin J-B, Olsson A, et al. Robust T cell immunity in convalescent individuals with asymptomatic or mild COVID-19. *bioRxiv* (2020) 06.29.174888. doi: 10.1101/2020.06.29.174888
17. Beura LK, Mitchell JS, Thompson EA, Schenkel JM, Mohammed J, Wijeyesinghe S, et al. Intravital mucosal imaging of CD8(+) resident memory T cells shows tissue-autonomous recall responses that amplify secondary memory. *Nat Immunol* (2018) 19(2):173–82. doi: 10.1038/s41590-017-0029-3
18. Park SL, Zaid A, Hor JL, Christo SN, Prier JE, Davies B, et al. Local proliferation maintains a stable pool of tissue-resident memory T cells after antiviral recall responses. *Nat Immunol* (2018) 19(2):183–91. doi: 10.1038/s41590-017-0027-5
19. Wakim LM, Waithman J, van Rooijen N, Heath WR, Carbone FR. Dendritic cell-induced memory T cell activation in nonlymphoid tissues. *Science* (2008) 319(5860):198–202. doi: 10.1126/science.1151869

20. Wein AN, McMaster SR, Takamura S, Dunbar PR, Cartwright EK, Hayward SL, et al. CXCR6 regulates localization of tissue-resident memory CD8 T cells to the airways. *J Exp Med* (2019) 216(12):2748–62. doi: 10.1084/jem.20181308
21. Agostini C, Cabrelle A, Calabrese F, Bortoli M, Scquizzato E, Carraro S, et al. Role for CXCR6 and its ligand CXCL16 in the pathogenesis of T-cell alveolitis in sarcoidosis. *Am J Respir Crit Care Med* (2005) 172(10):1290–8. doi: 10.1164/rccm.200501-142OC
22. Freeman CM, Curtis JL, Chensue SW. CC chemokine receptor 5 and CXC chemokine receptor 6 expression by lung CD8+ cells correlates with chronic obstructive pulmonary disease severity. *Am J Pathol* (2007) 171(3):767–76. doi: 10.2353/ajpath.2007.061177
23. Galkina E, Thatte J, Dabak V, Williams MB, Ley K, Braciale TJ. Preferential migration of effector CD8+ T cells into the interstitium of the normal lung. *J Clin Invest* (2005) 115(12):3473–83. doi: 10.1172/JCI24482
24. Kohlmeier JE, Miller SC, Smith J, Lu B, Gerard C, Cookenham T, et al. The chemokine receptor CCR5 plays a key role in the early memory CD8+ T cell response to respiratory virus infections. *Immunity* (2008) 29(1):101–13. doi: 10.1016/j.immuni.2008.05.011
25. Ray SJ, Franki SN, Pierce RH, Dimitrova S, Koteliansky V, Sprague AG, et al. The collagen binding alpha1beta1 integrin VLA-1 regulates CD8 T cell-mediated immune protection against heterologous influenza infection. *Immunity* (2004) 20(2):167–79. doi: 10.1016/s1074-7613(04)00021-4
26. Slutter B, Pewe LL, Kaech SM, Harty JT. Lung airway-surveilling CXCR3(hi) memory CD8(+) T cells are critical for protection against influenza A virus. *Immunity* (2013) 39(5):939–48. doi: 10.1016/j.immuni.2013.09.013
27. Hombrink P, Helbig C, Backer RA, Piet B, Oja AE, Stark R, et al. Programs for the persistence, vigilance and control of human CD8(+) lung-resident memory T cells. *Nat Immunol* (2016) 17(12):1467–78. doi: 10.1038/ni.3589
28. Kumar BV, Ma W, Miron M, Granot T, Guyer RS, Carpenter DJ, et al. Human Tissue-Resident Memory T Cells Are Defined by Core Transcriptional and Functional Signatures in Lymphoid and Mucosal Sites. *Cell Rep* (2017) 20 (12):2921–34. doi: 10.1016/j.celrep.2017.08.078
29. Mackay LK, Rahimpour A, Ma JZ, Collins N, Stock AT, Hafon ML, et al. The developmental pathway for CD103(+)CD8+ tissue-resident memory T cells of skin. *Nat Immunol* (2013) 14(12):1294–301. doi: 10.1038/ni.2744
30. Hogan RJ, Usherwood EJ, Zhong W, Roberts AA, Dutton RW, Harmsen AG, et al. Activated antigen-specific CD8+ T cells persist in the lungs following recovery from respiratory virus infections. *J Immunol* (2001) 166(3):1813–22. doi: 10.4049/jimmunol.166.3.1813
31. Wu T, Hu Y, Lee YT, Bouchard KR, Benechet A, Khanna K, et al. Lung-resident memory CD8 T cells (TRM) are indispensable for optimal cross-protection against pulmonary virus infection. *J Leukoc Biol* (2014) 95(2):215–24. doi: 10.1189/jlb.0313180
32. Zens KD, Chen JK, Farber DL. Vaccine-generated lung tissue-resident memory T cells provide heterosubtypic protection to influenza infection. *JCI Insight* (2016) 1(10):e85832. doi: 10.1172/jci.insight.85832
33. Strbo N, Pahwa S, Kolber MA, Gonzalez L, Fisher E, Podack ER. Cell-secreted Gp96-Ig-peptide complexes induce lamina propria and intraepithelial CD8+ cytotoxic T lymphocytes in the intestinal mucosa. *Mucosal Immunol* (2010) 3 (2):182–92. doi: 10.1038/mi.2009.127
34. Strbo N, Oizumi S, Sotosek-Tokmadzic V, Podack ER. Perforin is required for innate and adaptive immunity induced by heat shock protein gp96. *Immunity* (2003) 18(3):381–90. doi: 10.1016/S1074-7613(03)00056-6
35. Oizumi S, Strbo N, Pahwa S, Deyev V, Podack ER. Molecular and cellular requirements for enhanced antigen cross-presentation to CD8 cytotoxic T lymphocytes. *J Immunol* (2007) 179(4):2310–7. doi: 10.4049/jimmunol.179.4.2310
36. Selinger C, Strbo N, Gonzalez L, Aicher L, Weiss JM, Law GL, et al. Multiple low-dose challenges in a rhesus macaque AIDS vaccine trial result in an evolving host response that affects protective outcome. *Clin Vaccine Immunol* (2014) 21(12):1650–60. doi: 10.1128/CVI.00455-14
37. Strbo N, Garcia-Soto A, Schreiber TH, Podack ER. Secreted heat shock protein gp96-Ig: next-generation vaccines for cancer and infectious diseases. *Immunol Res* (2013) 57(1–3):311–25. doi: 10.1007/s12026-013-8468-x
38. Strbo N, Vaccari M, Pahwa S, Kolber MA, Doster MN, Fisher E, et al. Cutting edge: novel vaccination modality provides significant protection against mucosal infection by highly pathogenic simian immunodeficiency virus. *J Immunol* (2013) 190(6):2495–9. doi: 10.4049/jimmunol.1202655
39. Strbo N, Vaccari M, Pahwa S, Kolber MA, Fisher E, Gonzalez L, et al. Gp96 SIV Ig immunization induces potent polyepitope specific, multifunctional memory responses in rectal and vaginal mucosa. *Vaccine* (2011) 29(14):2619–25. doi: 10.1016/j.vaccine.2011.01.044
40. Savaraj N, Wu CJ, Xu R, Lampidis T, Lai S, Donnelly E, et al. Multidrug-resistant gene expression in small-cell lung cancer. *Am J Clin Oncol* (1997) 20 (4):398–403. doi: 10.1097/00000421-199708000-00016
41. Yamazaki K, Spruill G, Rhoderick J, Spielman J, Savaraj N, Podack ER. Small cell lung carcinomas express shared and private tumor antigens presented by HLA-A1 or HLA-A2. *Cancer Res* (1999) 59(18):4642–50.
42. Morgensztern D WS, Bazhenova L, McDermott L, Hutchins J, Yalor DH, Robinson FL, et al. Tumor antigen expression and survival of patients with previously-treated advanced NSCLC recieving viagenpumatucel-L (HS-110) plus nivolumab. *J Clin Oncol* (2020) 9546. doi: 10.1200/JCO.2020.38.15_suppl.9546
43. Yamazaki K, Nguyen T, Podack ER. Cutting edge: tumor secreted heat shock-fusion protein elicits CD8 cells for rejection. *J Immunol* (1999) 163 (10):5178–82.
44. Schenkel JM, Masopust D. Tissue-resident memory T cells. *Immunity* (2014) 41(6):886–97. doi: 10.1016/j.immuni.2014.12.007
45. Masopust D, Vezys V, Usherwood EJ, Cauley LS, Olson S, Marzo AL, et al. Activated primary and memory CD8 T cells migrate to nonlymphoid tissues regardless of site of activation or tissue of origin. *J Immunol* (2004) 172 (8):4875–82. doi: 10.4049/jimmunol.172.8.4875
46. Gonzalez L, Strbo N, Podack ER. Humanized mice: novel model for studying mechanisms of human immune-based therapies. *Immunol Res* (2013) 57(1–3):326–34. doi: 10.1007/s12026-013-8471-2
47. Vaccari M, Gordon SN, Fourati S, Schifanella L, Liyanage NP, Cameron M, et al. Adjuvant-dependent innate and adaptive immune signatures of risk of SIVmac251 acquisition. *Nat Med* (2016) 22(7):762–70. doi: 10.1038/nm.4105
48. van den Brand JM, Haagmans BL, van Riel D, Osterhaus AD, Kuiken T. The pathology and pathogenesis of experimental severe acute respiratory syndrome and influenza in animal models. *J Comp Pathol* (2014) 151 (1):83–112. doi: 10.1016/j.jcpa.2014.01.004
49. Kropp LE, Garg M, Binder RJ. Ovalbumin-derived precursor peptides are transferred sequentially from gp96 and calreticulin to MHC class I in the endoplasmic reticulum. *J Immunol* (2010) 184(10):5619–27. doi: 10.4049/jimmunol.0902368
50. Srivastava P. Roles of heat-shock proteins in innate and adaptive immunity. *Nat Rev Immunol* (2002) 2(3):185–94. doi: 10.1038/nri749
51. Binder RJ, Srivastava PK. Essential role of CD91 in re-presentation of gp96-chaperoned peptides. *Proc Natl Acad Sci USA* (2004) 101(16):6128–33. doi: 10.1073/pnas.0308180101
52. Messmer MN, Pasmowitz J, Kropp LE, Watkins SC, Binder RJ. Identification of the cellular sentinels for native immunogenic heat shock proteins in vivo. *J Immunol* (2013) 191(8):4456–65. doi: 10.4049/jimmunol.1300827
53. Yang ZY, Kong WP, Huang Y, Roberts A, Murphy BR, Subbarao K, et al. A DNA vaccine induces SARS coronavirus neutralization and protective immunity in mice. *Nature* (2004) 428(6982):561–4. doi: 10.1038/nature02463
54. Lai MMC, Holmes KV. *Fields Virology*. Philadelphia, PA: Lippincott Williams & Wilkins (2001).
55. Ni L, Ye F, Cheng ML, Feng Y, Deng YQ, Zhao H, et al. Detection of SARS-CoV-2-Specific Humoral and Cellular Immunity in COVID-19 Convalescent Individuals. *Immunity* (2020) 52(6):971–977 e3. doi: 10.1016/j.immuni.2020.04.023
56. Shane HL, Klonowski KD. Every breath you take: the impact of environment on resident memory CD8 T cells in the lung. *Front Immunol* (2014) 5:320:320. doi: 10.3389/fimmu.2014.00320
57. Liao M, Liu Y, Yuan J, Wen Y, Xu G, Zhao J, et al. Single-cell landscape of bronchoalveolar immune cells in patients with COVID-19. *Nat Med* (2020) 26 (6):842–4. doi: 10.1038/s41591-020-0901-9
58. Belyakov IM, Hammond SA, Ahlers JD, Glenn GM, Berzofsky JA. Transcutaneous immunization induces mucosal CTLs and protective immunity by migration of primed skin dendritic cells. *J Clin Invest* (2004) 113(7):998–1007. doi: 10.1172/JCI20261
59. del Rio ML, Bernhardt G, Rodriguez-Barbosa JII, Forster R. Development and functional specialization of CD103+ dendritic cells. *Immunol Rev* (2010) 234 (1):268–81. doi: 10.1111/j.0105-2896.2009.00874.x

60. Bedoui S, Whitney PG, Waithman J, Eidsmo L, Wakim L, Caminschi I, et al. Cross-presentation of viral and self antigens by skin-derived CD103+ dendritic cells. *Nat Immunol* (2009) 10(5):488–95. doi: 10.1038/ni.1724
61. Jozwik A, Habibi MS, Paras A, Zhu J, Guvenel A, Dhariwal J, et al. RSV-specific airway resident memory CD8+ T cells and differential disease severity after experimental human infection. *Nat Commun* (2015) 6:10224. doi: 10.1038/ncomms10224
62. McMaster SR, Wilson JJ, Wang H, Kohlmeier JE. Airway-Resident Memory CD8 T Cells Provide Antigen-Specific Protection against Respiratory Virus Challenge through Rapid IFN-gamma Production. *J Immunol* (2015) 195 (1):203–9. doi: 10.4049/jimmunol.1402975
63. Zhao J, Zhao J, Mangalam AK, Channappanavar R, Fett C, Meyerholz DK, et al. Airway Memory CD4(+) T Cells Mediate Protective Immunity against Emerging Respiratory Coronaviruses. *Immunity* (2016) 44(6):1379–91. doi: 10.1016/j.immuni.2016.05.006
64. Sun J, Dodd H, Moser EK, Sharma R, Braciale TJ. CD4+ T cell help and innate-derived IL-27 induce Blimp-1-dependent IL-10 production by antiviral CTLs. *Nat Immunol* (2011) 12(4):327–34. doi: 10.1038/ni.1996
65. Fisher E, Padula L, Podack K, O'Neill K, Seavey MM, Jayaraman P, et al. Induction of SARS-CoV-2 protein S-specific CD8+ T cells in the lungs of gp96-Ig-S vaccinated mice. *bioRxiv* (2020) 2020.08.24.265090. doi: 10.1101/2020.08.24.265090

Conflict of Interest: NS is inventor on the patent application No 62/983,783 entitled "Immune-mediated coronavirus treatments"; NS is a member of Heat Biologics COVID-19 Advisory Board. MS is the Executive Director of Special Projects. PJ is the Associate Director of Business Development, both are employed by Heat Biologics, Inc. RJ is the CEO of Pelican Therapeutics, a subsidiary of Heat Biologics, Inc. MS, PJ, RJ, and KP hold stock options in Heat Biologics, Inc.

The remaining authors declare that the research was conducted in the absence of any commercial or financial relationships that could be construed as a potential conflict of interest.